The Higgs Boson and the Top Quark

María Moreno-Llácer and Marcel Vos
IFIC (UV/CSIC) Valencia, Spain

Abstract

The Higgs boson and the top quark are the most massive elementary particles of the Standard Model, and their study is among the highest-priority goals of the program of the Large Hadron Collider. In this contribution, a brief review is presented of recent results in top physics from such accelerator, with emphasis on the many and strong connections of the top quark with the Higgs boson. The final sections review the bounds on the top-quark Yukawa coupling, its sign, and charge-parity structure, which have been derived using recent results.

Keywords: Higgs boson, top quark, large hadron collider, particle physics, high-energy colliders
DOI: 10.31526/LHEP.2023.453

1. INTRODUCTION

In the Standard Model of elementary particles and their interactions, matter is formed by spin 1/2 particles (fermions). The components of the atomic nucleus, protons and neutrons, are made up of three fermions charged under the strong interactions, which we call quarks. The structure formed by the up and down quarks, the electron, and the electron neutrino, which form ordinary matter, repeats itself in a second generation, with the strange and charm quarks, the muon and its corresponding neutrino, and a third generation quarks, with bottom and top quarks, the tau lepton, and its neutrino.

The quark model was built on the experimental discovery of a large number of composite particles, which could be explained as colour-neutral bound states of quarks and anti-quarks. The charm and bottom quark were observed in experiments in the 1970s, leaving only one quark to be discovered. The large mass of the top quark, however, prevented its observation at the installations that discovered the other quarks. The top quark escaped experimental scrutiny even at the most powerful proton-anti-proton and electron-positron colliders built in the 1980s. Only in 1995, the CDF and D0 experiments at the Tevatron proton-anti-proton collider at Fermilab could claim observation of the top quark [1, 2].

With a mass of approximately 173 GeV, the top quark is the heaviest elementary particle. This large mass implies that the top-quark Yukawa coupling must be of order one, much stronger than that of other fermions. This gives the top quark a close connection to the Higgs boson and a special role in the Standard Model. The top quark dominates the loop diagrams that enable Higgs boson production through gluon fusion and Higgs boson decay to photons, both crucial to the discovery of the Higgs boson [3, 4] by the ATLAS and CMS experiments at the Large Hadron Collider (LHC) at CERN in 2012.

Also in the new physics that lies beyond the Standard Model (and addresses a number of unexplained puzzles, from neutrino masses to dark matter), the top quark and Higgs boson are thought to play a key role. The top quark is responsible for large radiative corrections to the mass of the Higgs boson. Consequently, the top quark plays a special role in many extensions of the Standard Model inspired by the (unnatural?) hierarchy that keeps the Higgs boson light. Direct searches for undiscovered top partners have been performed in many scenarios, ranging from super-symmetry to composite Higgs models.

In this contribution to the special issue on the Higgs boson, we briefly review recent developments at the LHC with a focus on the interplay between top and Higgs physics.

2. TOP QUARKS AT HADRON COLLIDERS

Figure 1 shows representative Feynman diagrams for top-quark production at hadron colliders. Top quarks are predominantly produced in pairs at hadron colliders, through strong interaction. Top-quark pairs are selected cleanly in the dilepton and lepton+jets final states that result from the top quark decay to a W-boson and a bottom quark ($t \to Wb$), followed by a leptonic W-boson decay ($W \to l\nu_l$).

Importantly, the Standard Model predicts top-quark production rates precisely. Calculations for top-quark pair production have reached NNLO + NNLL precision [5]. This yields a prediction of the inclusive top-quark pair production cross section with a total uncertainty of about 4% at the LHC that can be confronted with measurements.

The $q\bar{q} \to t\bar{t}$ process is dominant at the Tevatron and drove the discovery of the top quark. The asymmetric $p\bar{p}$ collisions are particularly suited for measurements of the charge asymmetry [6] in top-quark pair production, which is readily observed as a forward-backward asymmetry of the order of 10%.

At the LHC, the dominant process is gluon-initiated $gg \to t\bar{t}$, while $q\bar{q} \to t\bar{t}$ accounts for about 10% at $\sqrt{s} = 13$ TeV. Cross-section measurements at the LHC have reached a precision well beyond what was thought feasible at a hadron collider, with inclusive cross-section measurements reaching a relative uncertainty of about 2% [7].

Beyond the inclusive production rate, top-quark pair production has been scrutinized in great detail, with differential cross-section measurements exploring a large number of observables. The LHC has explored center-of-mass energies from the production threshold to an invariant mass of the $t\bar{t}$ system up to several TeV, probing far into the high-energy regime, where the rest mass of the top quark is much smaller than its transverse momentum, and dedicated "boosted top" reconstruction techniques are required [8]. Analyses in fully hadronic final states, which must rely on jet-based trigger algorithms, are possible in this regime.

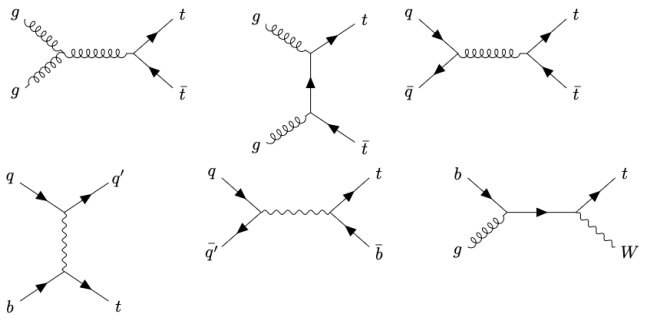

FIGURE 1: Feynman diagrams at leading-order for $t\bar{t}$ (top) and single-top-quark (bottom) production in hadron colliders. The first two $t\bar{t}$ diagrams are gluon-initiated and the last one corresponds to $q\bar{q}$ annihilation. For single-top-quark production, the three mechanisms are t-channel (left), s-channel (middle) and tW associated production (right).

3. EW INTERACTIONS OF THE TOP QUARK

The electroweak charged-current interactions of the top quark are precisely characterized [9]. Electroweak single-top production in the t-channel (i.e., $bq \to tq'$) and the s-channel ($qq' \to bt$) was observed at the Tevatron. ATLAS and CMS have observed the t-channel and associated production of a top quark in association with a $W-$boson ($gb \to tW$), but s-channel production remains elusive at the LHC. Strong bounds on the tWb vertex stem from precise measurements of top-quark decays, in particular from the measurements of the W-helicity fractions [10].

The top-quark interactions with the photon, the Z-boson and the Higgs boson, on the other hand, remained largely unexplored at the start of the LHC program. Associated top-quark production processes of a top-quark pair or a single-top quark with a boson, $pp \to t\bar{t}X$ and $pp \to tXq$ with $X = \gamma, Z, H$, provide direct constraints of the top-quark couplings with the photon (which is sensitive to the electric charge of the top quark), the Z-boson (sensitive to the weak isospin), and the Higgs boson (sensitive to the top-quark Yukawa coupling—much more on this crucial coupling later). These more complex associated production processes are known to NLO accuracy, with approximately 10% precision. Calculations at NNLO accuracy are becoming available for $t\bar{t}H$ [11] and $t\bar{t}W$ production [12].

The associated $t\bar{t}\gamma$, $t\bar{t}Z$, and $t\bar{t}W$ production processes were observed by ATLAS and CMS. A recent summary of results by the LHC Top Working Group is shown in Figure 2. The inclusive cross-section is measured to better than 10% precision after LHC Run 2, surpassing the precision of NLO predictions. Differential cross-section measurements have been performed for all three relatively rare processes. Also, $t\gamma q$ and tZq processes have been observed; their results are shown in the lower panel.

A systematic assessment of the electroweak couplings of the top quark can be made in the Standard Model Effective Field Theory (SMEFT), where the Standard Model Lagrangian is extended with all operators allowed by the Standard Model symmetries. In practice, phenomenological studies are limited to dimension-six operators in scenarios that severely limit the number of degrees of freedom due to flavor. A recent assessment of the top-quark electroweak couplings is provided in Figure 3 from [15] (based on earlier work by [14, 16]). The LHC measurements dominate the overall constraints, which reach $\mathcal{O}(1\,\text{TeV}^{-2})$ for most Wilson coefficients. The large number of orthogonal constraints from different processes is vital in global SMEFT fits that include a large number of degrees of freedom from $q\bar{q}t\bar{t}$ operators [17, 18].

4. $t\bar{t}H$ AND tH PRODUCTION

The Standard Model predicts many Higgs boson production processes of relevance at the LHC: gluon fusion $gg \to H$, vector-boson-fusion $q\bar{q} \to q\bar{q}H$, associated production with a vector boson $pp \to VH$, and associated production with a top-quark pair $pp \to t\bar{t}H$ or a single-top quark $pp \to tHq$. The latter two processes, shown in Figure 4, are the golden modes for measurements of the top-quark Yukawa coupling. The $t\bar{t}H$ cross section comprises only 1% of the total Higgs production at $\sqrt{s} = 13\,\text{TeV}$, with a production cross section of approximately 500 fb. In the case of tHq, this is about 75 fb [19].

The LHC experiments have observed all these production channels, combining a large number of decay modes: discovery channels $H \to ZZ^* \to 4l$ and $H \to \gamma\gamma$, $H \to WW^*$, $H \to \tau\tau$, and $H \to b\bar{b}$. Combining measurements in all production and decay modes, the LHC experiments can offer a complete characterization of its interactions [20, 21].

After the discovery of the Higgs boson, both ATLAS and CMS launched extensive searches for the $pp \to t\bar{t}H$ process, finally finding their reward in 2018 with the observation of the process by both experiments [22, 23]. It was important to target as many accessible experimental signatures as possible. The analysis channels for such complex final states can be separated in four classes according to the decays of the Higgs boson: $H \to ZZ^* \to 4l$ [24, 25], $H \to \gamma\gamma$ [26, 27], $H \to$ multileptons [28, 29, 30], and $H \to b\bar{b}$ [31, 32]. In each of these classes, the various decay final states of the top quarks are considered (fully hadronic, semileptonic, and dilepton decay final states).

The $H \to ZZ^* \to 4l$ decay channel ($l = e, \mu$) has a large signal-to-background ratio thanks to a low background rate and the complete reconstruction of the final state decay products, capitalizing on the excellent lepton momentum resolution of the LHC detectors. This analysis is currently limited by the low statistics due to the small branching fraction of the Z-boson decays to charged leptons.

The $H \to \gamma\gamma$ analysis relies on the search for a narrow mass peak in the $m_{\gamma\gamma}$ distribution. The background, mainly nonresonant diphoton production, is estimated from the $m_{\gamma\gamma}$ sidebands. The sensitivity in this channel is mostly limited by the available statistics.

The WW^*, $\tau\tau$, and ZZ^* final states are studied in multilepton event topologies (not including the resonant $H \to 4l$ that is covered in a more specific analysis as just discussed). Up to ten different experimental signatures are considered in the analyses, differing by the multiplicity of electrons, muons, and hadronically decaying tau leptons. These channels are further subdivided into event categories based on the multiplicity of jets and b-tagged jets or other properties of the leptons. The reconstruction of the Higgs boson is really difficult in these final states due to the missing neutrinos. The dominant backgrounds in most categories come from the production of top-quark pairs in association with W or Z-bosons. In the current results, the statistical and systematic uncertainties are of the same order.

The $H \to b\bar{b}$ decay channel, despite being the most probable in the Standard Model with a branching fraction of about

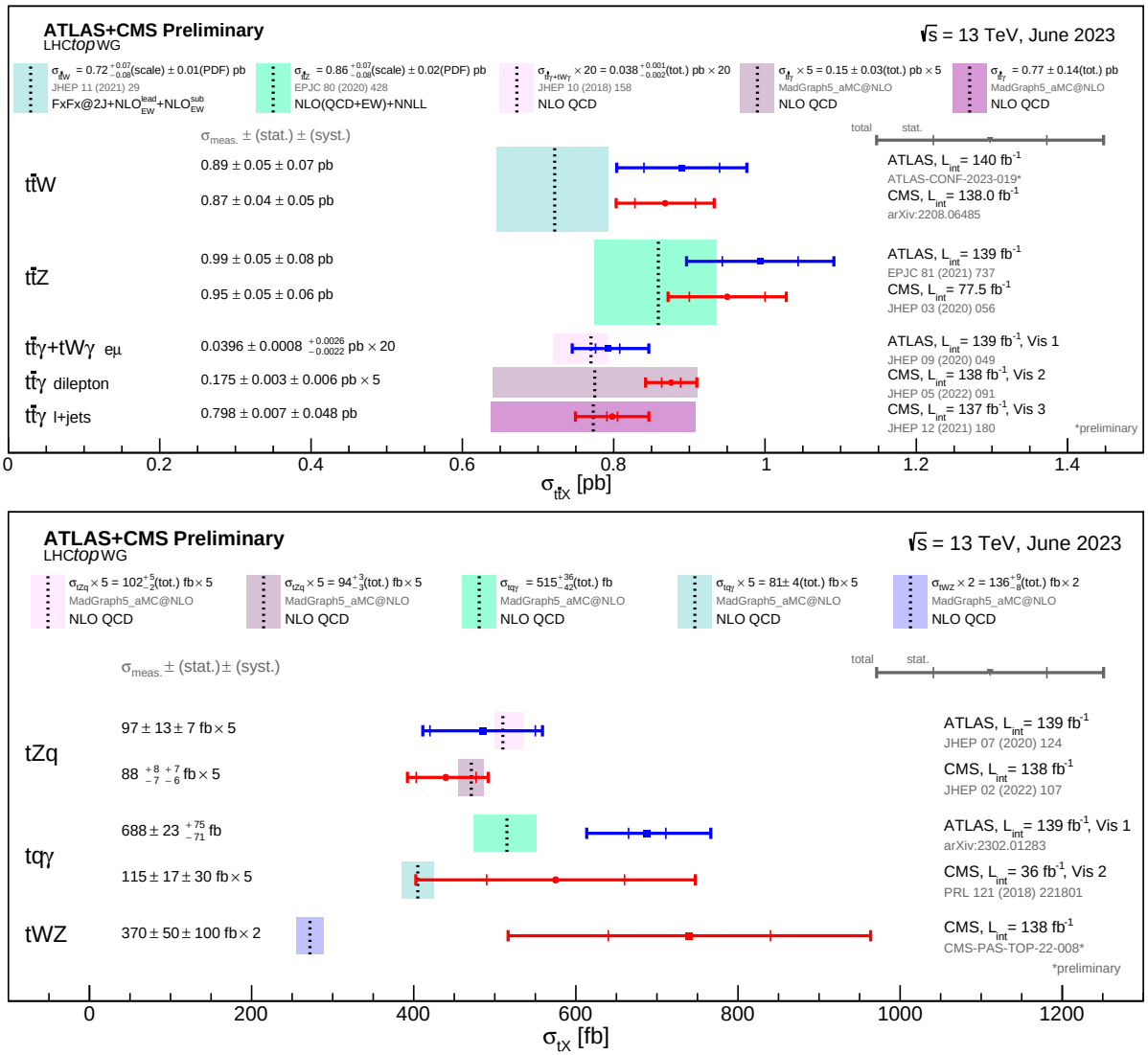

FIGURE 2: Summary plots of the LHC Top Working Group that collect the cross-section measurements for associated production processes with top quarks and gauge bosons: $pp \to t\bar{t}X$ in the upper panel and $pp \to tX$ in the lower panel. Source: [13].

58%, is intricate due to the large backgrounds, both physical and combinatorial in resolving the $b\bar{b}$ system from the Higgs boson decay. Already with the LHC Run 1 dataset, the sensitivity of this analysis was strongly impacted by the systematic uncertainties on the $t\bar{t}b\bar{b}$ background predictions. This channel is studied in a resolved mode, where the Higgs boson is reconstructed as two standard jets, and in a boosted mode, where it is reconstructed as a single large radius jet.

In most of these analyses, machine-learning techniques and/or matrix-element methods are applied to enhance the separation of signal over background processes. Events are classified into signal-enriched and background-enriched categories which are all included in a profile likelihood fit.

The combination of the measurements from the different channels for each experiment gives a $t\bar{t}H$ cross section consistent with the Standard Model prediction and with a precision of about 20%, with the statistical and systematic uncertainties of similar size. For the $H \to \gamma\gamma$ and $H \to b\bar{b}$ analyses, where the reconstruction of the Higgs boson is possible and there is sufficient statistics, measurements of the $t\bar{t}H$ cross section in several Higgs p_T bins, the so-called Simplified Template Cross Sections (STXS), are available. These are statistically limited in most of the phase space. The combination of Run 2 results of ATLAS and CMS would be beneficial.

One of the missing ingredients of the LHC Higgs program is the $pp \to tHq$ production process, where a single top quark is produced in association with a Higgs boson. ATLAS and CMS have produced specific searches for the tHq production mode exploiting a variety of Higgs boson decay modes: multileptonic decay signatures from the $H \to WW^*$, $H \to ZZ^*$, and $H \to \tau^+\tau^-$ decay modes, as well as $H \to b\bar{b}$ and $H \to \gamma\gamma$ channels [33, 29, 26]. These searches have not yet found evidence of the tHq process, with upper bounds on the production cross section of about 10 times the Standard Model prediction at a 95% confidence level (CL).

5. FOUR-TOP-QUARK PRODUCTION

The LHC Run 2 program for rare top-quark production processes culminates momentarily in the search for $pp \to t\bar{t}t\bar{t}$ pro-

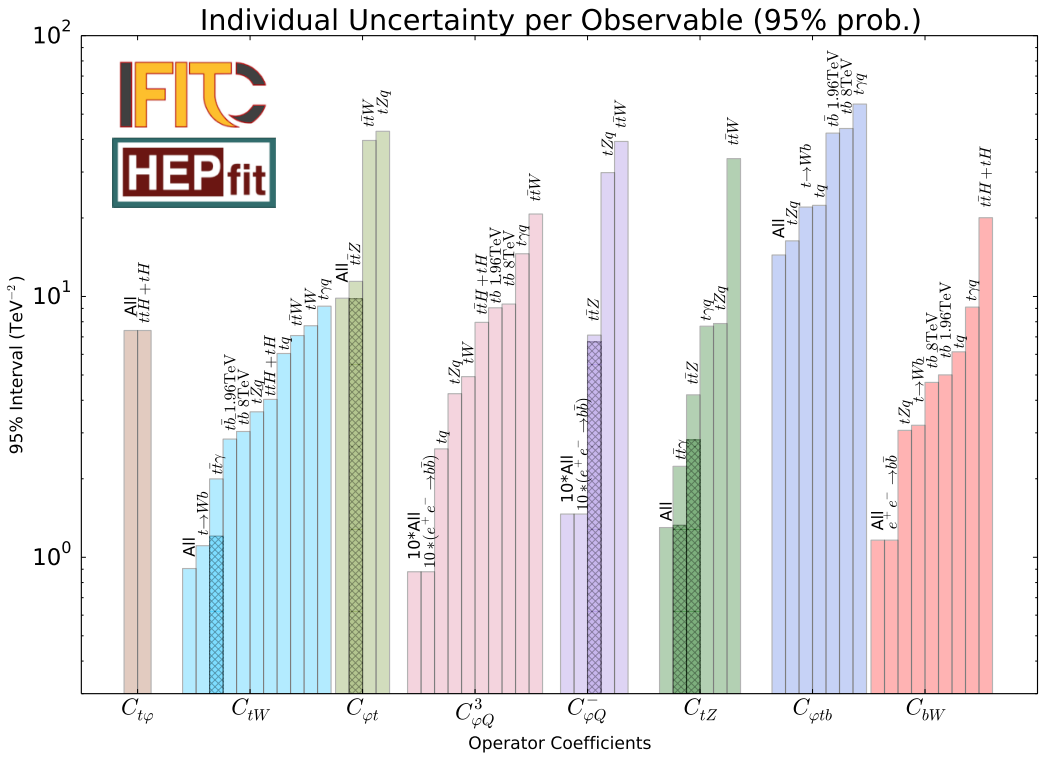

FIGURE 3: Individual 95% probability bounds on SMEFT operator coefficients that affect the top-quark electroweak couplings. The bounds are extracted from measurements by ATLAS and CMS at the LHC and from several legacy results by the LEP and Tevatron experiments. For each operator, the bounds are ordered from most to least constraining (going from left to right). Source: [14].

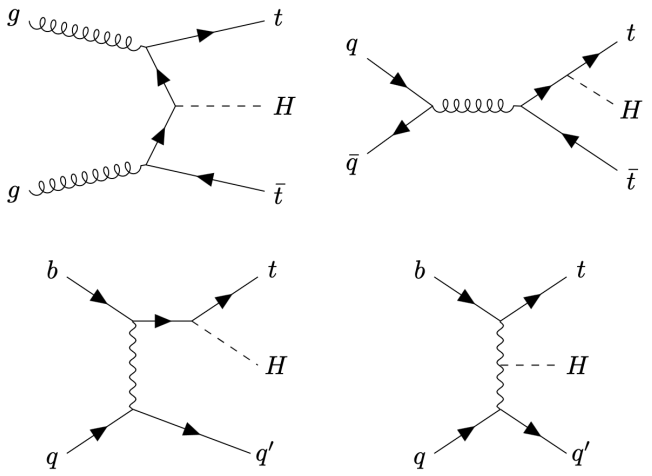

FIGURE 4: Example Feynman diagrams for $pp \to t\bar{t}H$ (top) and $pp \to tHq$ (bottom) production at hadron colliders. Top: The left diagram represents the production process initiated by gluons, while the initial state in the right diagram is formed by a quark-anti-quark pair. Bottom: The Higgs boson couples to the top quark in the left diagram and to the W-boson in the right one.

duction. With the rest masses of the four-top quarks adding up to 700 GeV, this process requires a very large center-of-mass energy to produce. Even at $\sqrt{s} = 13$ TeV the cross section in the Standard Model is only 13 fb [34], making it the rarest process observed at the LHC to date.

The most sensitive searches for four-top-quark production rely on same-sign lepton and multilepton signatures that are rare in Standard Model background processes, in combination with the excellent flavor tagging performance of the ATLAS and CMS experiments, to select the signal. Machine-learning and data-driven techniques are used to distinguish and control the rare top-quark production processes discussed in the previous section, which form the main background.

By the end of 2022, both experiments had found evidence for the four-top-production process in Run 2, with the observed significance exceeding 4σ, when combining different search channels (same-sign lepton + multilepton in ATLAS and all-hadronic in CMS). The search reached an apotheosis at the Moriond conference in March 2023, when both experiments independently announced observation [35, 36], with observed signal significance of 6.1σ (ATLAS) and 5.5σ (CMS).

A summary of the cross-section measurements by ATLAS and CMS is presented in Figure 5. In the most sensitive channels, both collaborations reach a precision of approximately 20%. The central result of both experiments is somewhat higher than the Standard Model prediction but remains within 2σ. The addition of Run 3 data and further refinements to the analyses will have to tell if the cross section is compatible with the Standard Model.

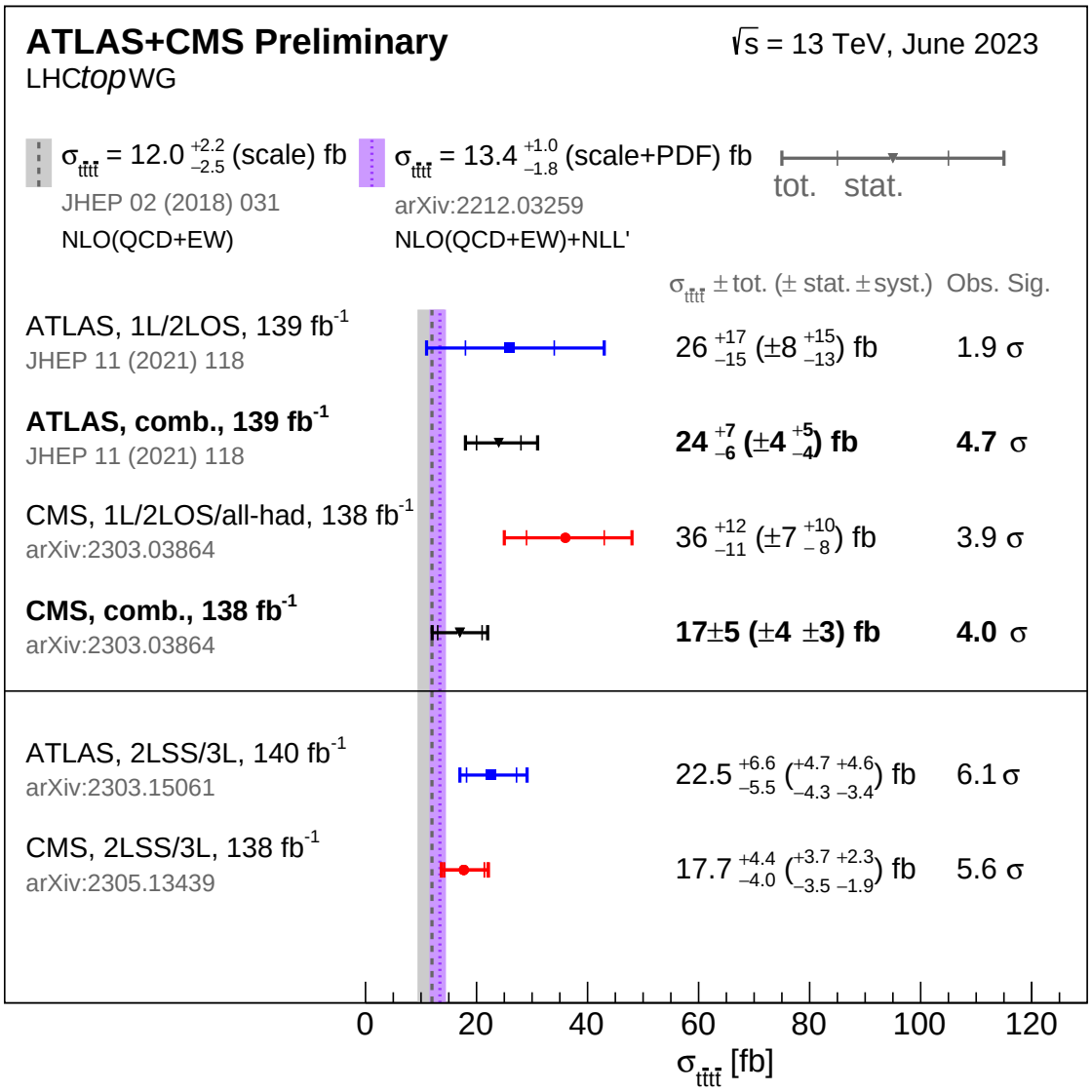

FIGURE 5: Summary plot of the LHC Top Working Group that collects the cross-section measurements for four-top-quark production processes. Source: [37].

6. THE TOP-QUARK YUKAWA COUPLING

The top-quark coupling to the Higgs boson is approximately 1 in the Standard Model and the strongest coupling in the theory. It hence offers a privileged window on the mechanism of electroweak symmetry breaking.

The absolute value of the top-quark Yukawa coupling is probed most directly in the associated production of a top-quark pair and a Higgs boson. The $pp \to t\bar{t}H$ cross section depends strongly on the Yukawa coupling in the Standard Model. Other SMEFT operators that affect the cross section can be probed to good precision in top-quark pair production and other associated production processes. The $t\bar{t}H$ cross section therefore provides a specific test of the top-Higgs interaction. The constraints on the coupling strength modifier κ_t obtained in two decay channels, $H \to b\bar{b}$ and $H \to$ multileptons, are indicated in Figure 6.

The top-Higgs coupling is implicitly present also in $gg \to H$ production and $H \to \gamma\gamma$ decay. Both processes proceed through loops, where the top-quark loop is the dominant contribution. These processes can provide quite powerful constraints when one assumes that the top-quark Yukawa coupling is the only parameter that can vary. The "resolved" result $\kappa_t = 1.01 \pm 0.09$ from $H \to \gamma\gamma$ indicated in red in Figure 6 is among the tightest bounds. In a more general scenario, the $gg \to H$ and $H \to \gamma\gamma$ rates depend on a large number of degrees of freedom (i.e., in the SMEFT operators that alter electroweak boson and top vertices) and the bounds prove to be less robust than those from $t\bar{t}H$ production. The upper marker in Figure 6 presents the bound of 0.94 ± 0.11 on the coupling modifier κ_t from the ATLAS Higgs fit in [20]. This result combines the different Higgs constraints.

The four-top production process is primarily mediated by the strong interaction. However, the electroweak process medi-

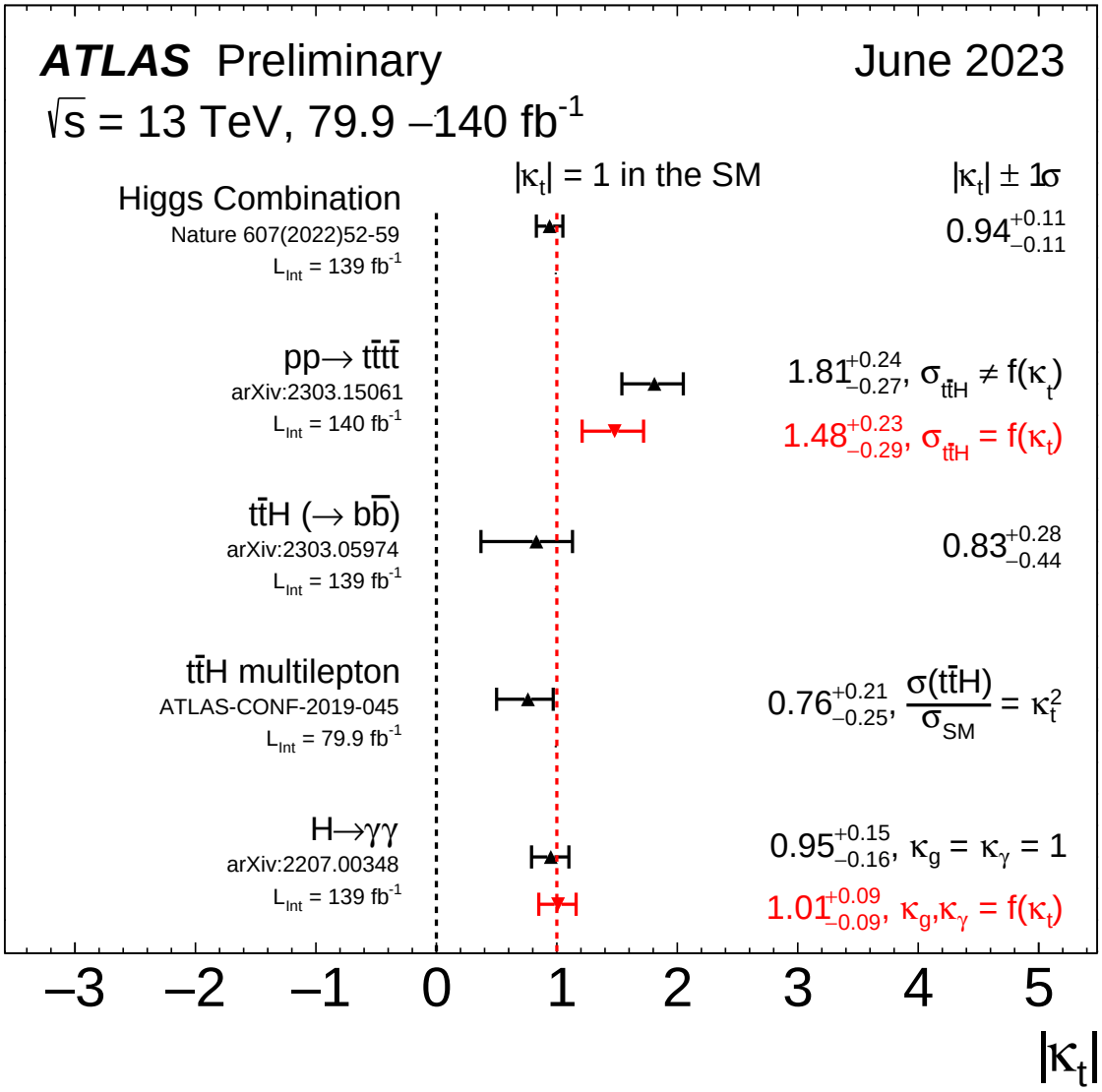

FIGURE 6: Summary of the ATLAS constraints on the coupling strength modifier κ_t that modifies the top-quark Yukawa coupling. The bounds derived from the $t\bar{t}H$ cross-section measurement in specific decay channels and from the $t\bar{t}t\bar{t}$ measurement are compared to the overall constraint from the Higgs fit in [20]. In some cases, alternative fits with a different assumption on the κ_t are indicated in red. Note: the regions are not explicitly orthogonal and bounds are therefore not independent. Source: [37].

ated by a Z/γ^* or Higgs boson has a sizable contribution and the overall $t\bar{t}t\bar{t}$ production rate has a nonnegligible dependence on the top-quark Yukawa coupling. A precise measurement of the four-top-quark production rate therefore gives an independent handle on the top-quark Yukawa coupling. The ATLAS experiment derived a 68% CL estimate of $\kappa_t = 1.48^{+0.23}_{-0.29}$ from the four-top-quark production cross section in [35]. While the central value is shifted by the slight excess in the measured $t\bar{t}t\bar{t}$ cross section, the relative precision of this orthogonal handle is competitive with that of each of the $t\bar{t}H$ analyses. The bound is complementary to those derived from Higgs analyses, as it does not depend on assumptions about Higgs boson branching fractions. This bound is indicated as the second point in Figure 6. The two results correspond to a fit where the top-quark-Yukawa-coupling dependence of the $t\bar{t}H$ background to four-top-quark production is parameterized along with the signal (in red) or ignored (in black). The latter indicates that most of the constraining power indeed comes from the $pp \to t\bar{t}t\bar{t}$ process itself.

The combination of the $t\bar{t}H$ and $t\bar{t}t\bar{t}$ cross sections can provide a measurement of the top-quark width [38].

A last independent handle on the top-quark Yukawa coupling can be obtained from a precision analysis of the top-quark pair production rate close to the production threshold at $m_{t\bar{t}} = 2m_t$. The cross section in this region is sensitive to virtual Higgs exchange between the top and anti-top quark and hence to the top-quark Yukawa coupling. The CMS analysis in [39] compares the observed production rate with a fixed-order pre-

diction that includes $\mathcal{O}(\alpha_s^2\alpha)$ electroweak corrections and finds a best-fit value of $\kappa_t = 1.07^{+0.34}_{-0.43}$ for the coupling modifier. An important caveat here is that the cross-section enhancement at the production threshold due to Coulomb interactions is not accounted for in the fixed-order calculation.

Due to the strong destructive interference of the two main leading-order diagrams for tHq production, this production mode is highly sensitive to the relative sign between the couplings of the Higgs boson to fermions and its couplings to gauge bosons. Recent searches for tHq production using the full LHC Run 2 dataset disfavor negative values of κ_t. The strongest constraint obtained by CMS is in the multilepton channel, where the only nonexcluded negative values of κ_t at 95% CL range between -0.9 and -0.7 [29]. The recent ATLAS $H \to \gamma\gamma$ results [26] lead to an exclusion of the $\kappa_t < 0$ region with a significance of 2.2σ.

7. CP STRUCTURE

Regarding the charge-parity (CP) structure of the top Yukawa, the Standard Model predicts a pure CP-even coupling, so an experimental observation compatible with the presence of a CP-odd term in the Higgs boson Lagrangian would be a direct indication of the presence of new physics. The ATLAS and CMS Collaborations studied the couplings of the Higgs boson to vector gauge bosons and also tested such interactions for CP violation using Run 1 data. All the studies were compatible with a pure CP-even Higgs boson, excluding pure CP-odd couplings of the Higgs boson to any of the gauge bosons. However, CP-violating effects are expected to be theoretically more motivated in fermionic couplings. In the couplings to bosons, CP-odd contributions enter via nonrenormalizable higher-order operators that are suppressed by powers of $1/\Lambda^2$, where Λ is the scale of the physics beyond the Standard Model. However, for the couplings to fermions, a renormalizable CP-violating coupling may instead occur at tree level. The top-Higgs Yukawa is therefore a suitable coupling for CP studies.

The SMEFT definition to introduce a CP-odd component in the top-Yukawa coupling is provided by the Higgs Characterization model [40, 41], which is implemented in the MadGraph5_aMC@NLO generator [42]. Within this model, the effective Lagrangian that describes the top-Yukawa coupling is expressed as

$$\mathcal{L} = -\bar{\psi}_t \left(c_\alpha \kappa_{Htt} g_{Htt} + i s_\alpha \kappa_{Att} g_{Att}\right) \psi_t X_0, \qquad (1)$$

where X_0 labels the scalar boson, $c_\alpha \equiv \cos(\alpha)$ and $s_\alpha \equiv \sin(\alpha)$ are related to the "CP mixing" parameters, $\kappa_{Htt,Att}$ are the dimensionless real coupling parameters, and $g_{Htt} = g_{Att} = m_t/v (= y_t/\sqrt{2})$, with $v \sim 246\,\text{GeV}$.

Defining $\kappa_t \cos(\alpha) = \kappa_{Htt} c_\alpha$ and $\kappa_t \sin(\alpha) = \kappa_{Att} s_\alpha$, it can be expressed as

$$\mathcal{L} = -\frac{m_t}{v} \bar{\psi}_t \kappa_t \left[\cos(\alpha) + i \sin(\alpha)\gamma_5\right] \psi_t X_0. \qquad (2)$$

The mixing angle $\alpha \in (-\frac{\pi}{2}, \frac{\pi}{2}]$ determines the relative strengths of the CP-even and CP-odd interactions. The Standard Model coupling corresponds to $\alpha = 0$ and $\kappa_t = 1$, while a fully CP-odd coupling is realized when $\alpha = \pi/2$.

The CP-odd component impacts the production rates and some kinematic distributions. Phenomenological studies [40] have shown that the tHq process is particularly enhanced in both the inverted coupling ($\kappa_t = -1$, $\alpha = 0$) and CP-odd case ($\alpha = \pi/2$). In cases where the Higgs boson is boosted, this enhancement is of a factor 10. The parameter α has been measured using $t\bar{t}H$ and tHq events in several decay modes obtaining that it is below 40° at 95% CL, being limited by data statistics. The scenario of pure CP-odd is excluded with more than 3σ by both experiments. In the $H \to \gamma\gamma$, $H \to ZZ^* \to 4l$, and $H \to$ multileptons, multivariate discriminants are used in order to distinguish CP-odd and CP-even states [43, 44, 45, 46]. In the $H \to b\bar{b}$ decay mode, dedicated CP-sensitive observables proposed in [47] have been explored experimentally [48].

The b_4 observable exploits the enhanced production of top quarks traveling in opposite longitudinal directions and closer to the beamline in the CP-odd case. The observable b_2 relies simultaneously on the smaller azimuthal separation of top quarks and on their larger longitudinal fraction of momentum in CP-odd $t\bar{t}H$ production. The calculation of b_2 is performed in the $t\bar{t}H$ rest frame [49], which enhances the discrimination power. Other novel observables have been proposed, such as the angle between the plane of incoming protons and the plane of the $t\bar{t}$ pair in the rest frame of the Higgs boson [50] and optimized linear combinations of variables [51, 52]. To define these observables, the reconstruction of the final state is required to maximize sensitivity, but this is quite challenging from the experimental side. New techniques and dedicated studies are crucial.

Measurements of electron and neutron dipole moments lead to tight constraints on the CP-odd component of the top-Higgs Yukawa coupling [53, 54] and measurements of these quantities have improved rapidly [55, 56, 57]. A combination of collider data, low-energy observables, and baryon asymmetry results is performed in [58].

Finally, the four-top-quark production process also has sensitivity to the CP structure of the top-quark Yukawa coupling through diagrams where the Higgs boson mediates the four-top-interaction. The bound derived from the ATLAS measurement of the four-top-quark production cross section is compared to the results of dedicated CP analyses in $t\bar{t}H$ production, with $H \to \gamma\gamma$ and $H \to b\bar{b}$ in Figure 7. The three analyses are found to be compatible with the Standard Model prediction at the 1-2σ-level.

8. TOP YUKAWA AND HIGGS SELF-COUPLING

The Higgs boson self-coupling is an extremely important direct probe of the Higgs potential with implications on our understanding of the electroweak phase transition. The Standard Model predicts that the Higgs boson couples to itself with a strength proportional to its mass.

The double Higgs boson production process gives access to the Higgs trilinear self-coupling, through the second diagram indicated in Figure 8. The first diagram shows the production mode of two Higgs bosons through a box diagram that involves mainly top quarks. This diagram offers no sensitivity to the trilinear self-coupling and is of similar importance in the Standard Model. The two diagrams interfere negatively, making the overall production rate smaller than what would be expected in the absence of a trilinear coupling.

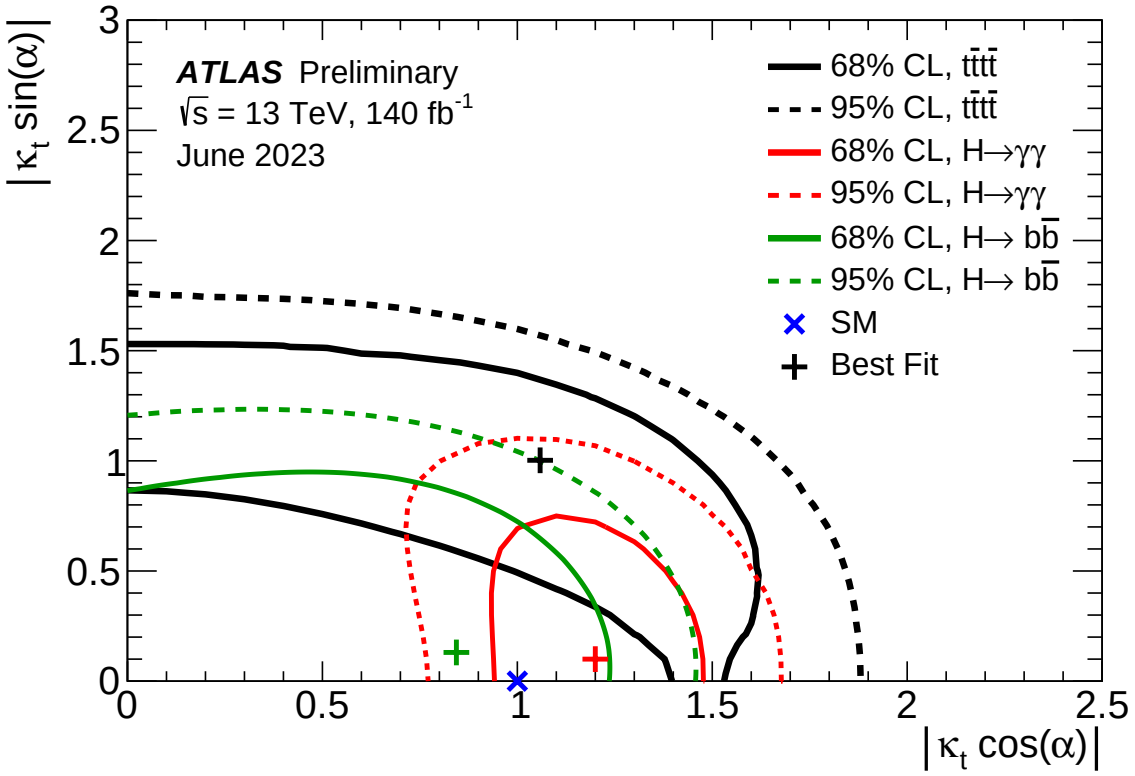

FIGURE 7: Summary of measurements by the ATLAS collaboration that constrain the coupling strength modifier κ_t of the top-quark Yukawa coupling and the CP mixing angle α (see equation (2) for the definition). The Standard Model prediction $\kappa_t = 1$ and $\alpha = 0$ is indicated with a blue cross. The best-fit results of the studies of the $H \to \gamma\gamma$ and $H \to b\bar{b}$ decays in $t\bar{t}H$ production as well as the four-top cross-section measurements are indicated with red, green, and black crosses, and the 68% and 95% CL areas with continuous and dashed lines of the same color. Source: [37].

A less direct constraint on the Higgs self-coupling can be derived from loop effects in single Higgs boson production. The double Higgs boson measurements yield stronger bounds. As they are dominated by statistical uncertainties, the di-Higgs bounds are expected to improve much more rapidly than the precision on single Higgs boson measurements.

The current 95% CL bounds on the Higgs self-coupling from ATLAS measurements are $-0.6 < \kappa_\lambda < 6.6$ [59]. Similar bounds are derived by CMS [21]. The ATLAS bounds degrade to $-1.4 < \kappa_\lambda < 6.1$ [59] if the coupling modifiers for the top and bottom quarks, the vector bosons, and the tau lepton are left free-floating. The interplay between the top-quark Yukawa coupling and the Higgs self-coupling plays a role in the di-Higgs constraint, but at the current precision, the freedom in κ_t does not limit the self-coupling measurement.

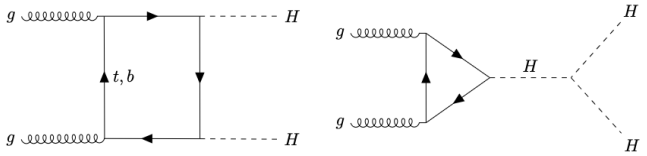

FIGURE 8: Feynman diagrams at leading-order for gluon-initiated double Higgs boson production in hadron colliders. The left diagram is proportional to the square of the top-quark Yukawa coupling, while the right one to the product of the top-quark Yukawa coupling and Higgs boson self-coupling.

9. BEYOND THE LHC

The LHC program still has a lot in store for the study of the Higgs boson and the top quark. After the completion of Run 3, which is scheduled to collect 300 fb^{-1} by the end of 2025, the luminosity upgrade of the LHC [60, 61] is to increase the instantaneous luminosity by nearly an order of magnitude. Over the next decade and a half, the ATLAS and CMS experiments are to collect 3 ab^{-1}, enabling precision measurements of the Higgs boson [62] and top quark [63]. In the κ-framework with coupling modifiers, the top-quark Yukawa coupling is expected to be determined to approximately 3-4% precision, where current determinations based on Run 2 data reach $\mathcal{O}(10\%)$ in each experiment [20, 21]. The result is dominated by associated $t\bar{t}H$ production [64].

The top quark and the Higgs boson are expected to remain among the most exciting forefront of high-energy physics also at the next large-scale facility [65, 64]. A new electron-positron collider operated at $\sqrt{s} = 240$–$250\,\text{GeV}$ can produce several million Higgs bosons through Higgs-strahlung ($e^+e^- \to ZH$). Higher-energy operation opens up vector-boson-fusion production of Higgs boson, top-quark pair production (for $\sqrt{s} > 2m_t$), and, eventually, di-Higgs boson production and $t\bar{t}H$ production (above $\sqrt{s} \sim 500\,\text{GeV}$). The Higgs factory phase at

$\sqrt{s} = 250\,\text{GeV}$ improves the measurements of all couplings to gauge boson and light fermions in an important way and provides sub-% indirect bounds on the top-quark Yukawa coupling from the $H \to \gamma\gamma$ and $H \to gg$ decay rates [66].

A scan of center-of-mass energy through the top-quark pair production threshold is foreseen in all e^+e^- collider projects and yields a measurement of the top-quark mass to approximately 50 MeV precision [67, 68, 69]. Constraints on top-quark electroweak couplings can be improved with measurements in top-quark pair production at several center-of-mass energies above the top-quark pair production threshold [16, 69]. A direct measurement of the top-quark Yukawa coupling [69] to a precision that exceeds the HL-LHC projection requires operation at a center-of-mass energy above 550 GeV and is therefore reserved for the energy upgrade of a linear collider.

A new hadron collider exploring the energy frontier [70] can provide a measurement of the top-quark Yukawa coupling in $t\bar{t}H$ production with negligible statistical uncertainty. The ultimate precision depends on the control of systematic and theory uncertainties. The use of cross-section ratios with respect to carefully chosen ancillary measurements (i.e., of $t\bar{t}H$ and $t\bar{t}Z$ production [71]) may offer an important handle for reducing systematic and theoretical uncertainties.

10. SUMMARY AND OUTLOOK

As the most massive Standard Model particle, the top quark is strongly coupled to the Higgs boson. An extensive program of measurements is ongoing to characterize the interactions of this enigmatic couple, in the hope of finding the keys to a deeper understanding of electroweak symmetry breaking. After the discovery of the Higgs boson in LHC in the first run of the LHC, operation at $\sqrt{s} = 13\,\text{TeV}$during 2015–2018 has opened up a large number of rare processes. The large center-of-mass energy yields cross sections of order (10–1000 fb) for processes with heavy gauge bosons and top quarks in the final state.

The measurements of these rare processes offer a new window on fundamental Standard Model parameters. In particular, the measurements of the $pp \to t\bar{t}H$ and $pp \to t\bar{t}Z$ cross sections have enabled a direct determination of the top-quark Yukawa and top-Z couplings. The recent observation of four-top-quark production offers yet another handle to constrain the top-quark Yukawa coupling. At the same time, dedicated CP analyses have the power to constrain its CP structure.

The high-luminosity phase of the LHC will push the precision of measurements of rare top quark and Higgs boson production processes. A new electron-positron collider operated above the top-quark pair production threshold can improve top-quark electroweak couplings.

CONFLICTS OF INTEREST

The authors declare that there are no conflicts of interest regarding the publication of this paper.

ACKNOWLEDGMENTS

This contribution reviews the measurements from ATLAS and CMS Collaborations from LHC at the CERN laboratory, and the authors are very grateful for their results. M. Moreno-Llácer acknowledges financial support from the Spanish Ministry of Science through the "Ramón y Cajal" grant RYC2019-028510-I, from the BBVA Foundation through a Leonardo Grant for Researchers in Physics (LEO22-1-603), and from the Generalitat Valenciana through the research project ASFAE/2022/010. The work of M. Vos is supported by PID2021-122134NB-C21, funded by the Spanish Ministry MCIN, and PROMETEO program (CIPROM/2021/073) of Generalitat Valenciana.

References

[1] CDF Collaboration, *Observation of top quark production in $\bar{p}p$ collisions*, *Phys. Rev. Lett.* **74** (1995) 2626 [hep-ex/9503002].

[2] D0 Collaboration, *Observation of the top quark*, *Phys. Rev. Lett.* **74** (1995) 2632 [hep-ex/9503003].

[3] ATLAS Collaboration, *Observation of a new particle in the search for the Standard Model Higgs boson with the ATLAS detector at the LHC*, *Phys. Lett. B* **716** (2012) 1 [1207.7214].

[4] CMS Collaboration, *Observation of a New Boson at a Mass of 125 GeV with the CMS Experiment at the LHC*, *Phys. Lett. B* **716** (2012) 30 [1207.7235].

[5] M. Czakon, P. Fiedler, and A. Mitov, *Total Top-Quark Pair-Production Cross Section at Hadron Colliders Through $O(\alpha_S^4)$*, *Phys. Rev. Lett.* **110** (2013) 252004 [1303.6254].

[6] J. A. Aguilar-Saavedra, D. Amidei, A. Juste, and M. Perez-Victoria, *Asymmetries in top quark pair production at hadron colliders*, *Rev. Mod. Phys.* **87** (2015) 421 [1406.1798].

[7] ATLAS Collaboration, *Inclusive and differential cross-sections for dilepton $t\bar{t}$ production measured in $\sqrt{s} = 13\,TeV$ pp collisions with the ATLAS detector*, 2303.15340.

[8] R. Kogler et al., *Jet Substructure at the Large Hadron Collider: Experimental Review*, *arXiv:1803.06991* **91** (2019) 045003.

[9] A. Giammanco and R. Schwienhorst, *Single top-quark production at the Tevatron and the LHC*, *Rev. Mod. Phys.* **90** (2018) 035001 [1710.10699].

[10] CMS, ATLAS Collaboration, *Combination of the W boson polarization measurements in top quark decays using ATLAS and CMS data at $\sqrt{s} = 8\,TeV$*, *JHEP* **08** (2020) 051 [2005.03799].

[11] S. Catani, S. Devoto, M. Grazzini et al., *Higgs Boson Production in Association with a Top-Antitop Quark Pair in Next-to-Next-to-Leading Order QCD*, *Phys. Rev. Lett.* **130** (2023) 111902 [2210.07846].

[12] L. Buonocore et al., *Associated production of a W boson with a top-antitop quark pair: next-to-next-to-leading order QCD predictions for the LHC*, 2306.16311.

[13] LHC Top Physics WG, *LSummary Plots*, *https://twiki.cern.ch/twiki/bin/view/LHCPhysics/LHCTopWGSummaryPlots*.

[14] V. Miralles et al., *The top quark electro-weak couplings after LHC Run 2*, *JHEP* **02** (2022) 032 [2107.13917].

[15] G. Durieux et al., *Snowmass White Paper: prospects for the measurement of top-quark couplings*, in *2022 Snowmass Summer Study*, 5, 2022 [2205.02140].

[16] G. Durieux et al., *The electro-weak couplings of the top and bottom quarks—Global fit and future prospects*, *JHEP* **12** (2019) 98 [1907.10619].

[17] SMEFiT Collaboration, *Combined SMEFT interpretation of Higgs, diboson, and top quark data from the LHC*, *JHEP* **11** (2021) 089 [2105.00006].

[18] J. Ellis, M. Madigan, K. Mimasu, V. Sanz, and T. You, *Top, Higgs, Diboson and Electroweak Fit to the Standard Model Effective Field Theory*, *JHEP* **04** (2021) 279 [2012.02779].

[19] LHC HIGGS CROSS SECTION WORKING GROUP Collaboration, *Handbook of LHC Higgs Cross Sections: 4. Deciphering the Nature of the Higgs Sector*, 1610.07922.

[20] ATLAS Collaboration, *A detailed map of Higgs boson interactions by the ATLAS experiment ten years after the discovery*, *Nature* **607** (2022) 52 [2207.00092].

[21] CMS Collaboration, *A portrait of the Higgs boson by the CMS experiment ten years after the discovery*, *Nature* **607** (2022) 60 [2207.00043].

[22] ATLAS Collaboration, *Observation of Higgs boson production in association with a top quark pair at the LHC with the ATLAS detector*, *Phys. Lett. B* **784** (2018) 173 [1806.00425].

[23] CMS Collaboration, *Observation of $t\bar{t}H$ production*, *Phys. Rev. Lett.* **120** (2018) 231801 [1804.02610].

[24] ATLAS Collaboration, *Higgs boson production cross-section measurements and their EFT interpretation in the 4ℓ decay channel at $\sqrt{s} = 13$ TeV with the ATLAS detector*, *Eur. Phys. J. C* **80** (2020) 957 [2004.03447].

[25] CMS Collaboration, *Measurements of production cross sections of the Higgs boson in the four-lepton final state in proton–proton collisions at $\sqrt{s} = 13$ TeV*, *Eur. Phys. J. C* **81** (2021) 488 [2103.04956].

[26] ATLAS Collaboration, *Measurement of the properties of Higgs boson production at $\sqrt{s} = 13$ TeV in the $H \to \gamma\gamma$ channel using 139 fb^{-1} of pp collision data with the ATLAS experiment*, 2207.00348.

[27] CMS Collaboration, *Measurements of Higgs boson production cross sections and couplings in the diphoton decay channel at $\sqrt{s} = 13$ TeV*, *JHEP* **07** (2021) 027 [2103.06956].

[28] ATLAS Collaboration, *Analysis of $t\bar{t}H$ and $t\bar{t}W$ production in multilepton final states with the ATLAS detector*, 2019.

[29] CMS Collaboration, *Measurement of the Higgs boson production rate in association with top quarks in final states with electrons, muons, and hadronically decaying tau leptons at $\sqrt{s} =$ 13 TeV*, *Eur. Phys. J. C* **81** (2021) 378 [2011.03652].

[30] ATLAS Collaboration, *Measurements of Higgs boson production cross-sections in the $H \to \tau^+\tau^-$ decay channel in pp collisions at $\sqrt{s} = 13$ TeV with the ATLAS detector*, *JHEP* **08** (2022) 175 [2201.08269].

[31] ATLAS Collaboration, *Measurement of Higgs boson decay into b-quarks in associated production with a top-quark pair in pp collisions at $\sqrt{s} = 13$ TeV with the ATLAS detector*, *JHEP* **06** (2022) 097 [2111.06712].

[32] CMS Collaboration, *Measurement of $t\bar{t}H$ production in the $H \to b\bar{b}$ decay channel in 41.5 fb^{-1} of proton-proton collision data at $\sqrt{s} = 13$ TeV*, 2019.

[33] CMS Collaboration, *Search for associated production of a Higgs boson and a single top quark in proton-proton collisions at $\sqrt{s} = 13$ TeV*, *Phys. Rev. D* **99** (2019) 092005 [1811.09696].

[34] M. van Beekveld, A. Kulesza, and L.M. Valero, *Threshold resummation for the production of four top quarks at the LHC*, 2212.03259.

[35] ATLAS Collaboration, *Observation of four-top-quark production in the multilepton final state with the ATLAS detector*, *arXiv:2303.15061* (2023) .

[36] CMS Collaboration, *Observation of four top quark production in proton-proton collisions at $\sqrt{s} = 13$ TeV*, 2305.13439.

[37] ATLAS Collaboration, *ATLAS Summary Plots*, https://atlas.web.cern.ch/Atlas/GROUPS/PHYSICS/PUBNOTES/ATL-PHYS-PUB-2023-013/ .

[38] Q.-H. Cao, S.-L. Chen, and Y. Liu, *Probing Higgs Width and Top Quark Yukawa Coupling from $t\bar{t}H$ and $t\bar{t}t\bar{t}$ Productions*, *Phys. Rev. D* **95** (2017) 053004 [1602.01934].

[39] CMS Collaboration, *Measurement of the top quark Yukawa coupling from $t\bar{t}$ kinematic distributions in the lepton+jets final state in proton-proton collisions at $\sqrt{s} = 13$ TeV*, *Phys. Rev. D* **100** (2019) 072007 [1907.01590].

[40] F. Demartin, F. Maltoni, K. Mawatari, B. Page, and M. Zaro, *Higgs characterisation at NLO in QCD: CP properties of the top-quark Yukawa interaction*, *Eur. Phys. J. C* **74** (2014) 3065 [1407.5089].

[41] F. Demartin, F. Maltoni, K. Mawatari, and M. Zaro, *Higgs production in association with a single top quark at the LHC*, *Eur. Phys. J. C* **75** (2015) 267 [1504.00611].

[42] J. Alwall et al., *The automated computation of tree-level and next-to-leading order differential cross sections, and their matching to parton shower simulations*, *JHEP* **07** (2014) 079 [1405.0301].

[43] ATLAS Collaboration, *CP Properties of Higgs Boson Interactions with Top Quarks in the $t\bar{t}H$ and tH Processes Using $H \to \gamma\gamma$ with the ATLAS Detector*, *Phys. Rev. Lett.* **125** (2020) 061802 [2004.04545].

[44] CMS Collaboration, *Measurements of $t\bar{t}h$ production and the CP structure of the yukawa interaction between the higgs boson and top quark in the diphoton decay channel*, *Phys. Rev. Lett.* **125** (2020) 061801.

[45] CMS Collaboration, *Constraints on anomalous higgs boson couplings to vector bosons and fermions in its production and decay using the four-lepton final state*, *Phys. Rev. D* **104** (2021) 052004.

[46] CMS collaboration, *Search for CP violation in ttH and tH production in multilepton channels in proton-proton collisions at $\sqrt{s} = 13$ TeV*, 2208.02686.

[47] J. F. Gunion and X.-G. He, *Determining the CP nature of a neutral Higgs boson at the LHC*, *Phys. Rev. Lett.* **76** (1996) 4468 [hep-ph/9602226].

[48] ATLAS Collaboration, *Probing the CP nature of the top-Higgs Yukawa coupling in $t\bar{t}H$ and tH events with $H \to b\bar{b}$ decays using the ATLAS detector at the LHC*, 2303.05974.

[49] A. Ferroglia, M .C. N. Fiolhais, E. Gouveia, and A. Onofre, *Role of the $t\bar{t}h$ rest frame in direct top-quark Yukawa coupling measurements*, *Phys. Rev. D* **100** (2019) 075034 [1909.00490].

[50] Q.-H. Cao, K.-P. Xie, H. Zhang, and R. Zhang, *A New Observable for Measuring CP Property of Top-Higgs Interaction*, *Chin. Phys. C* **45** (2021) 023117 [2008.13442].

[51] B. Bortolato, J.F. Kamenik, N. Košnik, and A. Smolkovič, *Optimized probes of CP-odd effects in the $t\bar{t}h$ process at hadron colliders*, *Nucl. Phys. B* **964** (2021) 115328 [2006.13110].

[52] D. A. Faroughy, J. F. Kamenik, N. Košnik, and A. Smolkovič, *Probing the CP nature of the top quark Yukawa at hadron colliders*, *JHEP* **02** (2020) 085 [1909.00007].

[53] J. Brod, U. Haisch, and J. Zupan, *Constraints on CP-violating Higgs couplings to the third generation*, *JHEP* **11** (2013) 180 [1310.1385].

[54] V. Cirigliano, W. Dekens, J. de Vries, and E. Mereghetti, *Is there room for CP violation in the top-Higgs sector?*, *Phys. Rev. D* **94** (2016) 016002 [1603.03049].

[55] ACME Collaboration, *Improved limit on the electric dipole moment of the electron*, *Nature* **562** (2018) 355.

[56] C. Abel et al., *Measurement of the Permanent Electric Dipole Moment of the Neutron*, *Phys. Rev. Lett.* **124** (2020) 081803 [2001.11966].

[57] T. S. Roussy et al., *A new bound on the electron's electric dipole moment*, 2212.11841.

[58] H. Bahl et al., *Constraining the $\mathcal{CP}$ structure of Higgs-fermion couplings with a global LHC fit, the electron EDM and baryogenesis*, *Eur. Phys. J. C* **82** (2022) 604 [2202.11753].

[59] ATLAS Collaboration, *Constraints on the Higgs boson self-coupling from single- and double-Higgs production with the ATLAS detector using pp collisions at $s = 13\,TeV$*, *arXiv:2211.01216* **843** (2023) 137745.

[60] I. Zurbano Fernandez et al., *High-Luminosity Large Hadron Collider (HL-LHC): Technical design report*, *CERN Yellow Rep. Monogr.* **10** (2020) [2020.0010].

[61] G. Apollinari, O. Brüning, T. Nakamoto, and L. Rossi, *High Luminosity Large Hadron Collider HL-LHC*, *CERN Yellow Rep.* (2015) 1 [1705.08830].

[62] M. Cepeda et al., *Report from Working Group 2: Higgs Physics at the HL-LHC and HE-LHC*, *CERN Yellow Rep. Monogr.* **7** (2019) 221 [1902.00134].

[63] P. Azzi et al., *Report from Working Group 1: Standard Model Physics at the HL-LHC and HE-LHC*, *CERN Yellow Rep. Monogr.* **7** (2019) 1 [1902.04070].

[64] R. K. Ellis et al., *Physics Briefing Book: Input for the European Strategy for Particle Physics Update 2020*, 1910.11775.

[65] M. Narain et al., *The Future of US Particle Physics - The Snowmass 2021 Energy Frontier Report*, 2211.11084.

[66] S. Boselli et al., *Prospects for the determination of the top-quark Yukawa coupling at future e^+e^- colliders*, *J. Phys. G* **46** (2019) 095005 [1805.12027].

[67] K. Seidel, F. Simon, M. Tesar, and S. Poss, *Top quark mass measurements at and above threshold at CLIC*, *Eur. Phys. J. C* **73** (2013) 2530 [1303.3758].

[68] M. Vos et al., *Top physics at high-energy lepton colliders*, 1604.08122.

[69] K. Agashe et al., *Report of the Topical Group on Top quark physics and heavy flavor production for Snowmass 2021*, 2209.11267.

[70] FCC Collaboration, *FCC-hh: The Hadron Collider: Future Circular Collider Conceptual Design Report Volume 3*, *Eur. Phys. J. ST* **228** (2019) 755.

[71] M. Mangano et al., *Measuring the Top Yukawa Coupling at 100 TeV*, *J. Phys. G* **43** (2016) 035001 [1507.08169].